ELSEVIER

Nuclear Instruments and Methods in Physics Research A 435 (1999) 102–108

NUCLEAR INSTRUMENTS & METHODS IN PHYSICS RESEARCH Section A

www.elsevier.nl/locate/nima

The CMS silicon strip tracker

E. Focardi[a,*], S. Albergo[b], M. Angarano[c], P. Azzi[d], E. Babucci[e], N. Bacchetta[d], A. Bader[c], G. Bagliesi[c], P. Bartalini[e], A. Basti[f], U. Biggeri[a], G.M. Bilei[e], D. Bisello[d], D. Boemi[b], F. Bosi[f], L. Borrello[f], C. Bozzi[f], S. Braibant[g], H. Breuker[g], M. Bruzzi[a], A. Candelori[d], A. Caner[g], R. Castaldi[f], A. Castro[d], E. Catacchini[a], B. Checcucci[e], P. Ciampolini[e], C. Civinini[a], D. Creanza[c], R. D'Alessandro[a], M. Da Rold[d], N. Demaria[g], M. de Palma[c], R. Dell'Orso[f], R. Della Marina[h], S. Dutta[f], C. Eklund[k], A. Elliott-Peisert[g], L. Feld[g], L. Fiore[c], M. French[i], K. Freudenreich[h], A. Fürtjes[g], A. Giassi[f], A. Giraldo[d], B. Glessing[g], W.H. Gu[j], G. Hall[k], R. Hammerstrom[g], T. Hebbeker[l], J. Hrubec[m], M. Huhtinen[g], A. Kaminsky[d], V. Karimaki[n], St. Koenig[j], M. Krammer[m], P. Lariccia[e], M. Lenzi[a], M. Loreti[d], K. Luebelsmeyer[j], W. Lustermann[h], P. Mättig[g], G. Maggi[c], M. Mannelli[g], G. Mantovani[e], A. Marchioro[g], C. Mariotti[g], G. Martignon[d], B. Mc Evoy[k], M. Meschini[a], A. Messineo[f], S. My[c], A. Paccagnella[d], F. Palla[f], D. Pandoulas[m], G. Parrini[a], D. Passeri[e], M. Pieri[a], S. Piperov[l], R. Potenza[b], F. Raffaelli[f], G. Raso[m], M. Raymond[k], A. Santocchia[e], B. Schmitt[i,1], G. Selvaggi[c], L. Servoli[e], G. Sguazzoni[f], R. Siedling[j], L. Silvestris[c], K. Skog[n], A. Starodumov[f], I. Stavitski[d], G. Stefanini[g], P. Tempesta[c], G. Tonelli[f], A. Tricomi[b], T. Tuuva[o], C. Vannini[f], P.G. Verdini[f], G. Viertel[h], Z. Xie[f], Y. Wang[e], S. Watts[p], B. Wittmer[j]

[a] *INFN sez. di Firenze and Università di Firenze, Firenze, Italy*
[b] *INFN sez. di Catania and Università di Catania, Catania, Italy*
[c] *INFN sez. di Perugia and Università di Perugia, Perugia, Italy*
[d] *INFN sez. di Padova and Università di Padova, Padova, Italy*
[e] *INFN sez. di Bari and Università di Bari, Bari, Italy*
[f] *INFN sez. di Pisa and Università di Pisa, Pisa, Italy*
[g] *CERN, European Laboratory for Particle Physics, Geneva, Switzerland*
[h] *Laboratory for High Energy Physics, ETH, Zurich, Switzerland*
[i] *Helsinki Institute of Physics, Helsinki, Finland*
[j] *Rutherford Appleton Laboratory, Didcot, UK*
[k] *I. Physikalisches Institut, RWTH, Aachen, Germany*
[l] *Imperial College, UK*
[m] *Humboldt University, Berlin, Germany*
[n] *Institut fur Hochenergiephysik der OeAW, Wien, Austria*

* Corresponding author.
E-mail address: focardi@fi.infn.it (E. Focardi)
[1] Now at Philips, Zurich, Switzerland.

0168-9002/99/$ - see front matter
PII: S0168-9002(99)00585-9

[o]University of Oulu, Kemi, Finland
[p]Brunel University, Middlesex, UK

Abstract

The Silicon Strip Tracker (SST) is the intermediate part of the CMS Central Tracker System. SST is based on microstrip silicon devices and in combination with pixel detectors and the Microstrip Gas Chambers aims at performing pattern recognition, track reconstruction and momentum measurements for all tracks with $p_T \geq 2$ GeV/c originating from high luminosity interactions at $\sqrt{s} = 14$ TeV at LHC. We aim at exploiting the advantages and the physics potential of the precise tracking performance provided by the microstrip silicon detectors on a large scale apparatus and in a much more difficult environment than ever. In this paper we describe the actual SST layout and the readout system.

PACS: 29.40. – Gx

Keywords: SST; CMS apparatus

1. Introduction

The CMS apparatus [1] aims at cleanly detecting the different signatures of new physics at LHC by identifying and precisely measuring muons, electrons, photons and jets over a large energy range. Experience has shown that a robust tracking and a detailed vertex reconstruction within a strong magnetic field are powerful tools for this purpose. The characterization of events involving gauge bosons, W and Z and in particular, their leptonic decays provide clean experimental signals. To fully exploit these signatures the Central Tracker has to provide a good momentum measurement for energetic leptons. The tracker measurements are combined with track segments reconstructed in the outer muon system to extend the kinematic region of a precise muon momentum measurement. Several physics channel studies imply an efficient isolated lepton reconstruction. A key requirement will be to keep to a minimum the material budget in order to have photon conversion close to 50%. Within the expected CMS Tracker performance we have good impact parameter resolution in the transverse plane (35 μm) and in the longitudinal direction (75 μm) over most of the rapidity range for particles with $p_T > 10$ GeV/c [2,3]. One of the critical issues of the SST is the long-term survival after heavy irradiation. The system has to be designed to guarantee stable operating conditions for about 10 years of LHC running. In this period the most irradiated detector of the SST will be subjected to an average fluence of 1.6×10^{14} 1-MeV-equivalent neutrons/cm^2.

2. Detector description

The SST consists of 70 m^2 of instrumented silicon strip detectors subdivided in a barrel region with five cylindrical layers plus six mini-disks and two end-cap regions each one composed of ten disks, Fig. 1. The SST covers the radial region between 22 and 60 cm. In the barrel part each layer is equipped with rectangular detectors providing r–ϕ information: layers 1, 2 and 5 also deliver small-angle stereo measurements for the z-coordinate. The mini-disks are equipped with wedge-shaped detectors and provide r–ϕ and radial measurements. The end-cap disks are made-out of four concentric rings of wedge-shaped detectors. Disks 1–6 on each side are fully instrumented with four rings; disks 7 and 8 are equipped with 3 outer rings and disks 9 and 10 with two outer rings. In each disk rings 1 and 4 provide double-sided information while rings 2 and 3 are single-sided. The SST extends longitudinally for about 5.6 m and covers the pseudorapidity region $|\eta| \leq 2.5$. Each

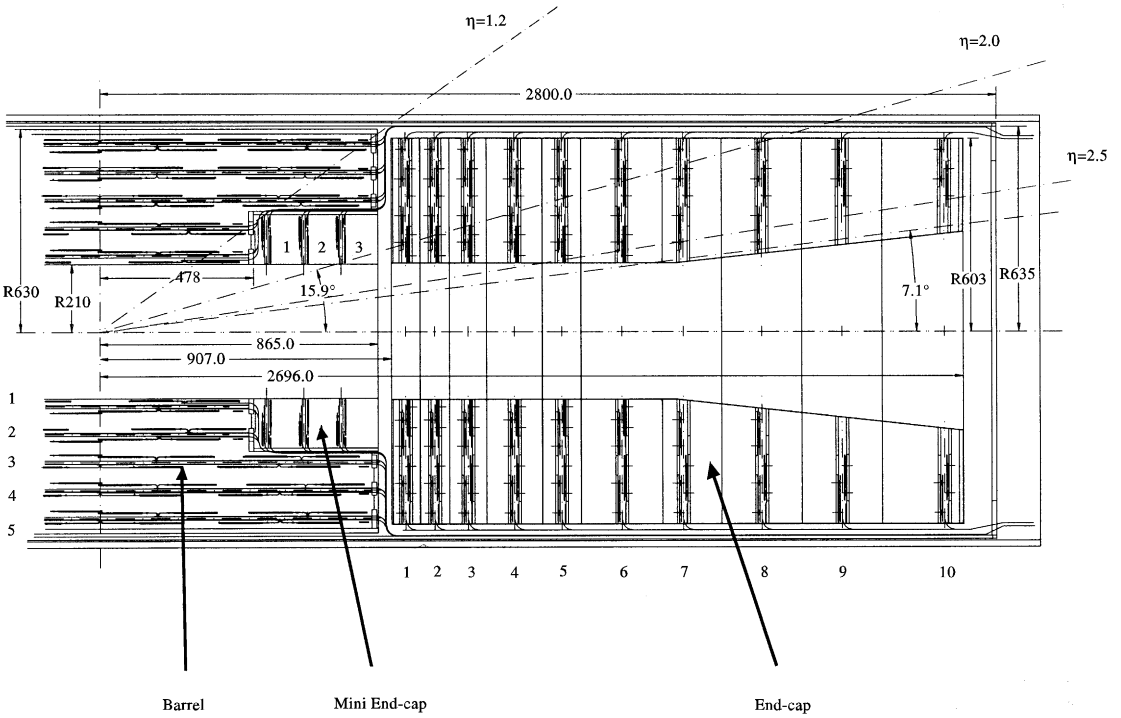

Fig. 1. SST longitudinal view.

Silicon sensor is 300 μm thick and is read-out by the front-end electronics at a pitch varying between 60 and 270 μm. The sensors will be based on the use of single-sided p^+ patterned-implants in an initially n-type bulk silicon [4]. The capability of reading different coordinates is reached by coupling two such sensors back-to-back. The silicon detectors, 18 500 in total, are assembled in modules with strip lengths ranging from 7 to 12.5 cm. The barrel modules are tilted by 9° to compensate for the Lorentz angle and are arranged to allow ϕ and z overlap to avoid dead regions. The modules, fabricated by using 6.4×6.4 cm^2 Si detectors, are fixed to the mechanical structure by using positioning pins, Fig. 2; to allow easy assembly and disassembly the detector modules are positioned on both sides of each supporting cylindrical element. Each layer is made of two half cylinders which can be independently assembled, surveyed and tested before rigidly connecting together. 1372 single-sided and 1364 double-sided (back-to-back sensors) modules will

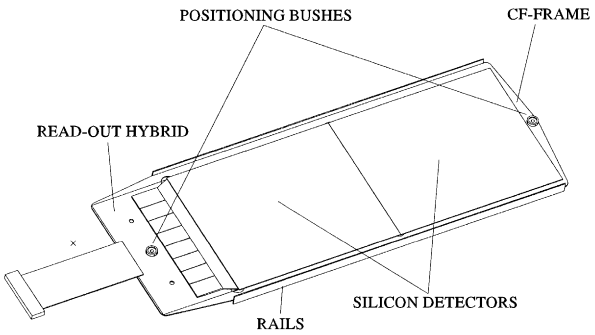

Fig. 2. Single-sided barrel module.

be used to equip the cylindrical layers of the barrel part. Each disk of the mini end-cap is equipped with two rings of wedge-shaped modules: each ring houses 36 modules and one module has a pair of silicon sensors, the front one with radial strips and the back one with stereo strips. The six disks of the

mini end-cap contain 432 modules. A perspective view of the barrel detector is shown in Fig. 3. At both the ends of the barrel region 10 disks are placed to obtain full coverage and to optimize the track reconstruction performance in the pseudo-rapidity region $1.2 \leq |\eta| \leq 2.5$. To permit overlapping the wedge-shaped modules are mounted alternately on the two sub-disks of which each disk is composed and within each ring the detector modules are mounted alternately on both sides of a pair of supporting rings, Fig. 4. The end-cap detector consists of 3168 modules (1548 r–ϕ, 1620 stereo). To achieve the expected measuring accuracy the detector modules have to be held in place by a low-mass rigid structure. Shells of high modulus carbon fiber composites ($\sim$ 500 GPa) are foreseen for the mechanical structure that incorporates an efficient cooling system, able to maintain the SST temperature at -10°C. The cooling system will be based on fluids used to cool by direct conduction all elements producing power and cold dry nitrogen circulated through the system. A thermal shield will isolate the SST and the pixel detector volume from the outside detectors operated at room temperature. Each module will be fabricated with an internal precision of 5 μm in the detector plane and 30 μm orthogonally to this plane. The absolute initial position of each strip will be known with an accuracy better than 10 μm. The maximum displacements from the nominal positions will be kept below 100 μm and the stability with time under stable operating conditions will be at the level of 10 μm.

3. Readout system

Each SST strip is read out by a charge sensitive amplifier followed by a shaper with 50 ns peaking time; its output voltage is sampled at the beam crossing rate (40 MHz). The samples are stored in the cells of an analogue pipeline for the maximum Level 1 trigger latency of 3.2 μs. After Level 1, a deconvolution of the nominal shaper response

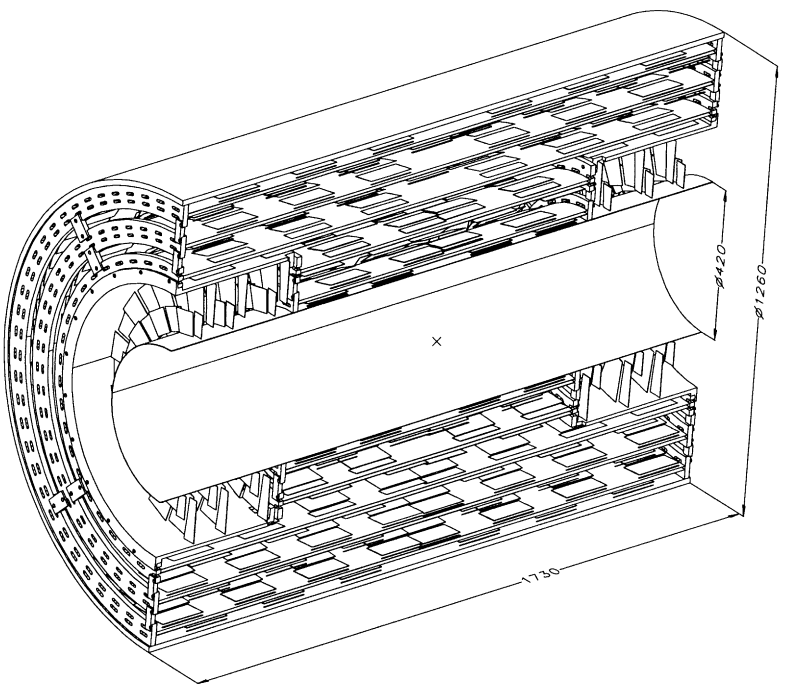

Fig. 3. Perspective view of the barrel detector.

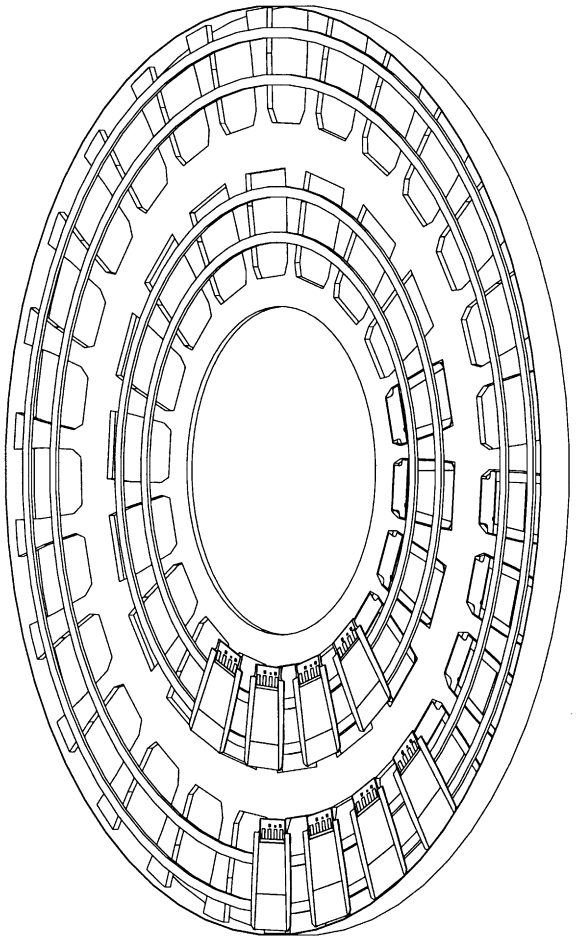

Fig. 4. End-cap sub-disk partially assembled.

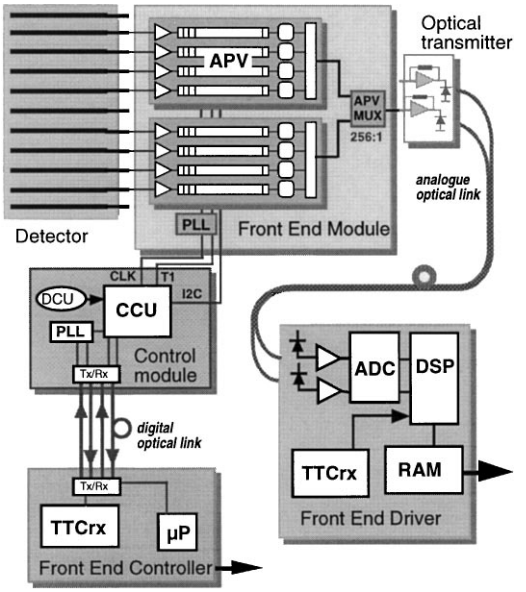

Fig. 5. A schematic representation of the tracker readout and control system.

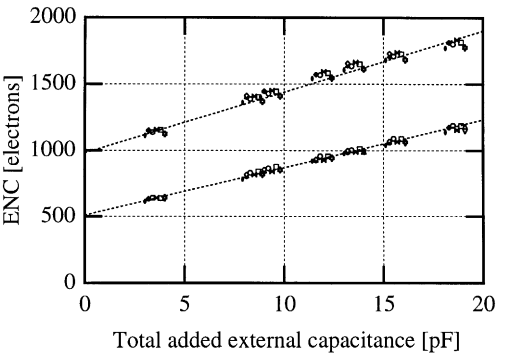

Fig. 6. APV6 equivalent noise charge dependence on the input capacitance in peak mode (bottom) and deconvolution mode (top).

can be performed to recover the single bunch crossing–timing accuracy. The analogue data are then multiplexed, converted to analogue optical signals and brought through optical fibers to the Front-End Driver (FED) boards, the VME-based digitizer electronics. The choice of the analogue data readout is driven by the reduction of the front-end chip complexity, power dissipation and potentially better position resolution through charge sharing between strips. A schematic of the read-out system is shown in Fig. 5. The total number of analogue channels to be read-out is 5.2×10^6. The front-end chip, APV6, has 128 analogue inputs; after receiving a trigger for each channel a series of samples from the pipeline is fed through a filter (APSP) capable of deconvoluting the shaper response to the sampled data. The output is given either by the peak amplitude of the shaper output for that trigger (peak mode) or by the peak amplitude as reshaped by APSP (deconvolution mode), recovering the single crossing timing but paying with an increased noise. The equivalent noise charge dependence on input capacitance is given by $510e^- + 36e^-/pF$ in peak mode and $1000e^- + 46e^-/pF$ in deconvolution mode, Fig. 6. With 12.5 cm as maximum strip

length we expect to have a S/N ratio of 12:1 at the end of the detector lifetime. An additional memory buffer holds the data before transmission via the output analogue multiplexer operating at 20 MHz. The current output of the APV varies from 0 to + 600 μA; the baseline offset is adjustable to maximize the dynamic range and the m.i.p. signal will be equivalent to a current of 50 μA. Apart from the APV chips themselves the front-end hybrids house a few components like decoupling capacitors, connectors, chips used to recover locally the clock signals and the quadruple 2:1 multiplexer chip (APVMUX). The optical fibers carrying the data from the APV chips will be connected to the FED digitizing boards that convert data to electrical levels by a 10 bit flash ADC. Dedicated circuitry will perform strip reordering and pedestal subtraction. Each 9 unit VME-bus module contains 64 channels of conversion and digitization together with the pre-processing circuitry. The optical transmission of the analogue data at 40 Msamples/s reduces the electrical interference, minimizes the material budget for cables and reduces power dissipation, Fig. 7. The system is multi-way unidirectional based on edge-emitting laser transmitters (Tx) coupled to single-mode optical fibers, multiway MT connectors and pin-photodiode receivers (Rx). The operational wavelength is $\lambda \sim 1310$ nm. To allow for testing, installation and maintenance of the system, three breakpoints are foreseen, two within the detector and one on the receiving/driving electronics. The expected performance of the front-end electronics coupled with prototype sensors has been investigated. Fig. 8 shows the result of a calculation superimposed on the beam test data. The two curves correspond to the variation of the input parameters of the calculation within their experimental uncertainties.

4. Conclusion

The apparatus described here is the result of several years of dedicated effort in developing

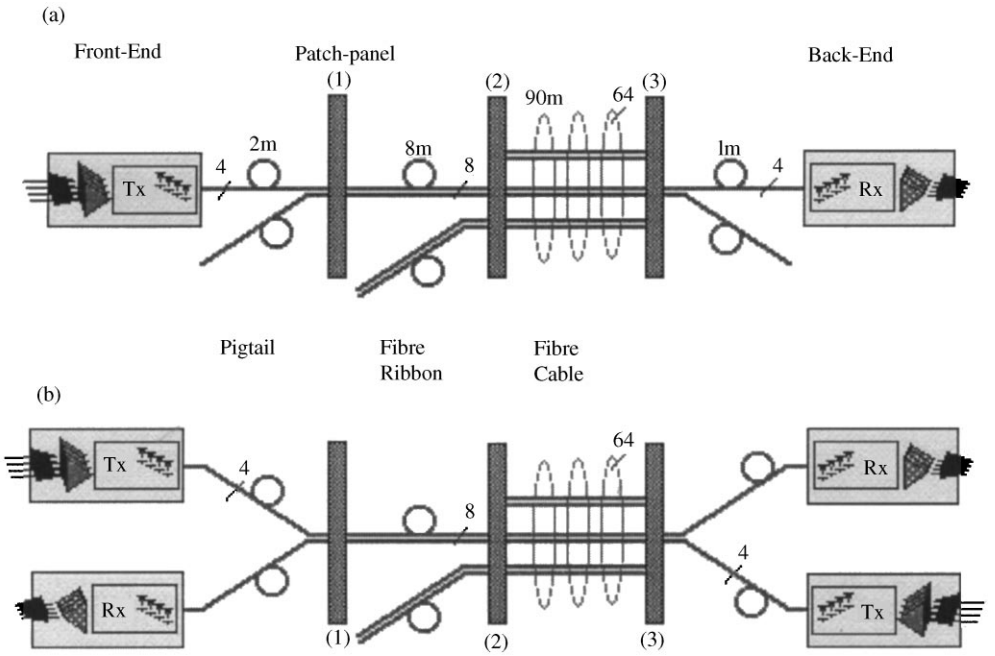

Fig. 7. A layout of the optical systems foreseen for the CMS-Tracker: (a) analogue readout, (b) digital control and timing distribution.

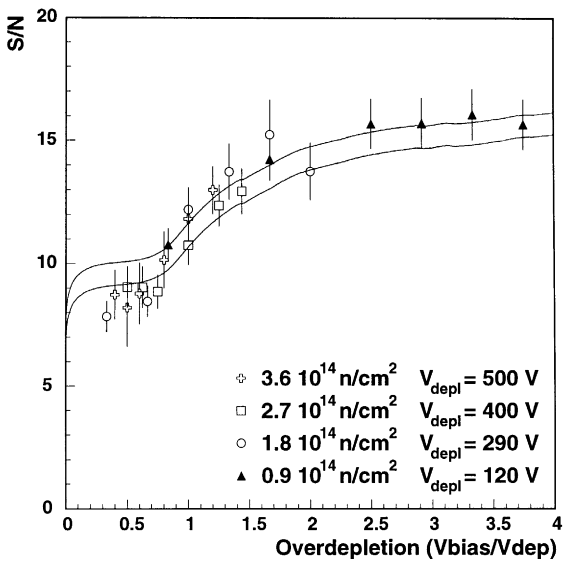

Fig. 8. The predicted S/N ratio (no deconvolution) after irradiation versus bias voltage, in over-depletion units. The experimental results are superimposed.

radiation resistant detectors and electronics, including the fabrication of small systems. Before starting the construction we plan to conclude the sensors and electronics development and to finalize the fabrication procedures both for the modules and the support structures. The actual production phase will start during the year 2000.

References

[1] CMS Collaboration, Technical Proposal, CERN/LHC 94-38.
[2] CMS Collaboration, The Tracker Project, Technical Design Report, CERN/LHCC 98-6.
[3] A. Caner, Nucl. Instr. and Meth. A 435 (1999) 118.
[4] G. Tonelli, Nucl. Instr. and Meth. A 435 (1999) 109.